Unravelling the Intrinsic Reactivity and Colloidal Instability in Tin-Based Halide Perovskite Precursor Solutions

Jorge Pascual,[*,#,a,b] Marion Flatken,[#,c] Eros Radicchi,[d] Mahmoud Aldamasy,[c] Shuaifeng Hu,[*,e] Omar E. Solis,[f] Silver-Hamill Turren-Cruz,[f] Guixiang Li,[g] Armin Hoell,[c] Susan Schorr,[c] Meng Li,[h] Filippo De Angelis,[i,j] Artem Musiienko,[c] André Dallmann,[k] Antonio Abate[*,c,l,m]

[a] Instituto de Tecnología Química, Universitat Politècnica València-Consejo Superior de Investigaciones Científicas, Av. dels Tarongers, 46022 València, Spain

[b] Polymat, University of the Basque Country UPV/EHU, 20018 Donostia-San Sebastian, Spain

[c] Helmholtz-Zentrum Berlin für Materialien und Energie, Hahn-Meitner-Platz 1, 14109 Berlin, Germany

[d] Department of Engineering DIMI, University of Verona, Strada Le Grazie 15, 37134, Verona, Italy

[e] Clarendon Laboratory, Department of Physics, University of Oxford, Oxford, UK

[f] Instituto Universitario de Ciencia de los Materiales (ICMUV), Universitat de València, Paterna, Spain

[g] School of Materials Science and Engineering, Southeast University, Nanjing, Jiangsu, 211189 China

[h] Key Lab for Special Functional Materials, Ministry of Education, National & Local Joint Engineering Research Center for High-efficiency Display and Lighting Technology, School of Materials Science and Engineering, and Collaborative Innovation Center of Nano Functional Materials and Applications, Henan University, Kaifeng 475004, China

[i] Department of Chemistry, Biology and Biotechnology, University of Perugia, Via Elce di Sotto 8, 06123, Perugia, Italy

[j] SKKU Institute of Energy Science and Technology (SIEST), Sungkyunkwan University, Suwon 440-746, South Korea

[k] Humboldt Universität zu Berlin, Institut für Chemie, AG NMR, Germany

[l] Department of Chemical Materials and Industrial Production Engineering, University of Naples Federico II, Piazzale Tecchio 80, Napoli, Italy

[m] Department of Chemistry Bielefeld University, Universitätsstraße 25, Bielefeld, 33615, Germany

Corresponding Author

Jorge Pascual, jpasmie@itq.upv.es

Shuaifeng Hu, shuaifeng.hu@physics.ox.ac.uk

Antonio Abate, antonio.abate@helmholtz-berlin.de

ORCID ID's

Jorge Pascual: 0000-0001-6486-0737

Marion Flatken: 0000-0003-2653-4468

Eros Radicchi: 0000-0003-0749-3824

Mahmoud Aldamasy: 0000-0003-3331-5570

Shuaifeng Hu: 0000-0003-1312-075X

Omar E. Solis: 0000-0003-3590-8716

Silver-Hamill Turren-Cruz: 0000-0003-3191-6188

Guixiang Li: 0000-0002-8730-0713

Armin Hoell: 0000-0002-7080-8393

Susan Schorr: 0000-0002-6687-614X

Meng Li: 0000-0003-0360-7791

Filippo De Angelis: 0000-0003-3833-1975

Artem Musiienko: 0000-0002-2259-8387

André Dallmann: 0000-0002-0141-2635

Antonio Abate: 0000-0002-3012-3541

Author Contributions

# These authors contributed equally.

KEYWORDS: tin halides, perovskite solar cells, lead-free, colloids, crystallization, NMR, small-angle X-ray scattering

Abstract

Narrow-bandgap tin and mixed tin–lead halide perovskites are attracting growing interest for optoelectronic applications, yet the difficult-to-control crystallization process has hindered their development. Although additive engineering has effectively improved film formation, the fundamental origins of their distinct crystallization behavior remain less explored. Here, through direct comparison with Pb counterparts, we investigate the pre-crystallization stages of Sn-based perovskite precursor solutions through complementary structural characterizations. We show that Sn precursors are intrinsically more reactive and sensitive to their chemical environment, exhibiting poorer colloidal stability compared to Pb and a strong inherent tendency to agglomerate. These findings explain their narrower processing window, where small variations in solution chemistry strongly affect nucleation and crystallization dynamics. To fabricate high-quality tin-based perovskite through solution methods, we highlight the importance of controlling the often overlooked pre-crystallization stages, through, for example, rational solvent and additive designs. In addition, we provide fundamental insights into precursor solution chemistry and establish pre-crystallization engineering as a key strategy for overcoming long-standing limitations in thin-film fabrication, particularly in light of the field's rapid progression toward large-scale, sustainable, and solvent-conscious manufacturing.

Introduction

One of the primary advantages of metal halide perovskites is their high compositional versatility with a wide range of structural and optoelectronic properties.[1] With ABX_3 structure, Sn^{2+} and Pb^{2+} have been the most prominent perovskite B-site metal cations, particularly for their application in solar cells.[2-3] In particular, tin-containing perovskites, with energy gaps as low as ~1.2 eV[4-5] and minimal ion migration,[6-9] hold potential for overcoming the performance of lead-based materials or even the Shockley-Queisser efficiency limit through multijunction technologies.[10-11] However, the introduction of tin in the structure also brings in inconveniencies linked to its redox stability and the limited processing options.[12-13] In particular, the more delicate fabrication of tin-based perovskites entails lower quality thin films with irreproducibility issues and high defect content, hampering their development and applicability.

The field has made significant progress in understanding tin-based perovskite crystallization, largely based on the rapid transition from solution to the black perovskite phase without "stable" solvent/metal halide-based intermediates, generally observed for Pb-based perovskites.[14-16] Over time, this phenomenon has been ascribed to fast nucleation and crystal growth rates,[17-20] driven by the higher reactivity of tin halides with A-site salts due to the higher acidity of Sn^{2+} species and their lower solubility in the strongly binding dimethyl sulfoxide (DMSO). Building on this understanding, the community systematically employed additives that coordinate strongly with Sn^{2+} centers, essentially Lewis bases, aimed to moderate the reaction rate between tin halides and A-site components during perovskite formation.[21-22] Recent studies have highlighted the critical role of colloidal characteristics in tin-based perovskites, influencing both precursor evolution and the resulting quality of the crystallized thin films.[23-25] Other works also discuss the mismatch between the crystal structures of tin halide intermediates and perovskites and their implications in the crystallization mechanism.[26-27] However, direct experimental evidence supporting the assumed reaction pathways is still limited, and studies capturing the detailed transition from solution to thin films remain scarce, leaving the pre-crystallization stages less explored. Thus, the current understanding remains insufficient to explain fundamentally the distinct mechanisms governing tin and lead species, which is essential for establishing highly reproducible and tolerant fabrication protocols enabling the further development of these materials.

In this work, we address these fundamental gaps by investigating the unique reactivity and colloidal characteristics of tin perovskite precursor solutions, comparing them to their lead-based counterparts. Here, we use the term "pre-crystallization stage" to describe the solution-state regime preceding nucleation, in which metal halide complexes and A-site cations form pre-nucleation clusters (PNCs) through progressive association and short-range organization that preconditions the subsequent crystallization process. With the combination of NMR and small-angle X-ray scattering (SAXS) characterization of the precursor solutions, we provide a detailed picture of the unique reactivity and colloidal characteristics of tin perovskites.

We prepare MI_2 and $FAMI_3$ (FA: formamidinium) solutions in *N*,*N*-dimethylformamide (DMF) and DMSO at varying concentrations and characterize them using ^{119}Sn and ^{207}Pb NMR. Detailed interpretation of NMR spectra in Supporting Information, all data in Figure S2-6, Table S1-4. We measure the NMR spectra of SnI_2, PbI_2, $FASnI_3$ and $FAPbI_3$ precursor solutions at 1.0 M

(Figure 1a). We plot ^{119}Sn and ^{207}Pb NMR data together in the same graph for practical reasons. First, we investigate the change in chemical shift from MI_2 to $FAMI_3$. In DMF, $FASnI_3$ presents a downfield change of 391 ppm with respect to SnI_2, while $FAPbI_3$ shows an increase of 741 ppm from PbI_2. This change in the chemical shift to higher values implies a decrease in the electronic density around the metals, reasonable considering that the A-site component promotes the association of the perovskite precursors and the interaction between iodidometallates.[28-31] As a consequence, the degree of coordination by iodide around the metal increases, displacing the solvent that has a stronger electron-donating ability than iodide, thus overall decreasing the electronic density around tin and lead nuclei. For DMSO solutions, the change from PbI_2 to $FAPbI_3$ shows a comparable downfield change of 753 ppm in the chemical shift. However, the value of $FASnI_3$ only increases by 81 ppm. Thus, DMSO binds Sn^{2+} very strongly, to the point that it greatly impedes the A-site salt-driven pre-arrangement of tin precursors in solution, which does not occur for lead. We note that liquid-state NMR provides an ensemble-averaged signal, so the observed chemical shifts reflect the combined contributions of multiple coexisting coordination species in solution and not just a single $[MI_n]^{2-n}$ iodidometallate species. We carried out calculations evaluating the relative interaction energies (E_{rel}) of PbI_2/SnI_2/$FAPbI_3$/$FASnI_3$ with the solvents (DMSO, DMF), as per the following equation:

$$E_{rel} = E_{tot} - E_{iodido} - E_{solv}$$

where E_{tot} is the total energy of the PbI_2/SnI_2/$FAPbI_3$/$FASnI_3$ solvated system, E_{iodido} the energy of the unsolvated system, and E_{solv} the energy of the solvent molecule. These results confirm the stronger solvation of Sn^{2+} by the solvents, and the stronger influence of the reactivity of the A-site cation with this metal, despite being countered by DMSO (Figure 1b). Calculated structures are available in Figure S7. These findings also agree with the observations by Yang et al., where the desorption barrier of DMSO from tin is larger than from lead.[27]

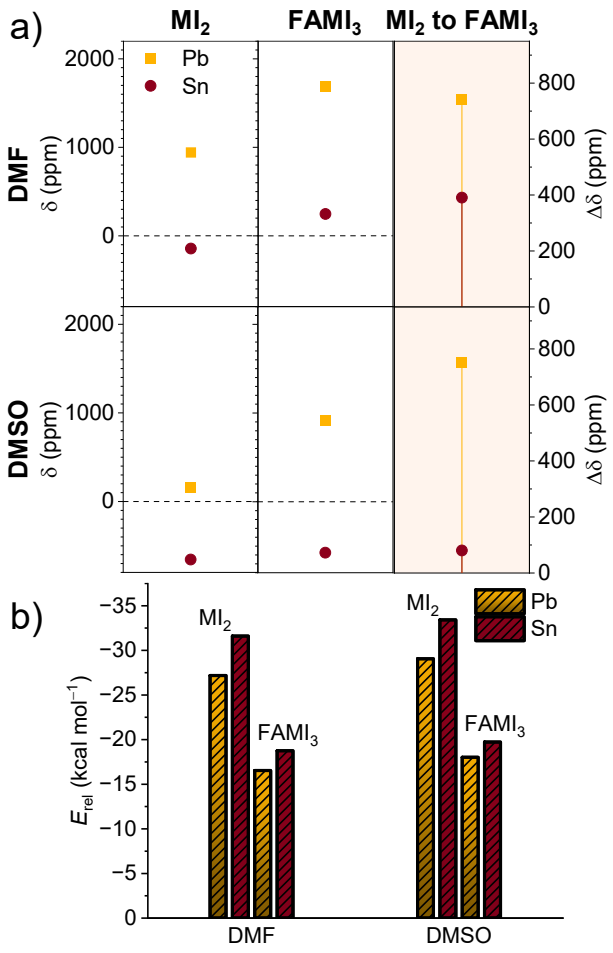

Figure 1. ^{119}Sn and ^{207}Pb NMR of perovskite precursor solutions. a) Influence of solvent and A-site salt on the chemical shift. b) Calculated binding strength of solvents to the different precursors.

We measure the sensitivity of the environment of SnI_2 to varying amounts of FAI (Figure 2a). In DMF, the chemical shift of SnI_2 increases linearly and already significantly at sub-stoichiometric values, saturating at a 1:1 mixture. However, in DMSO SnI_2 does not vary relevantly, and only increases to a more significant extent in the presence of an excess of 2.0 equivalents of FAI (-457.8 ppm), still not comparable to DMF (282.2 ppm). These results evidence the exceptional ability of DMSO to inhibit tin perovskite pre-arrangement. In fact, the chemical shift change from DMF to DMSO for $FASnI_3$ (-821 ppm) is even greater than for $FAPbI_3$ (-772 ppm), even considering the broader frequency range of Pb nucleus in NMR. These results underscore that tin precursors are significantly more sensitive to solution composition and processing conditions than robust Pb^{2+} systems.

In addition, we analyze the sensitivity of tin precursors in the different solvents at varying concentrations (Figure 2b). Tin environment shows minimal concentration dependence in DMF, particularly for SnI_2. In DMSO, both SnI_2 and $FASnI_3$ exhibit a notable initial increase of chemical shift at low concentrations (0.01-0.2 M), then a less pronounced linear increase. Thus, DMSO solvates Sn^{2+} much more effectively at high dilution conditions, but becomes slightly less effective at higher solute concentrations. This strong solvation at low concentrations is evidenced by the almost negligible chemical shift change from SnI_2 to $FASnI_3$ (Figure 2c). However, under higher solute presence, this difference becomes more relevant, evidencing that A-site cation starts to compete with DMSO for metal coordination, while still negligible compared to DMF, showing chemical shift changes of 350-400 ppm even at low concentrations. These findings align with the expectation that unequal competition between solvent and anion will make chemical shift values deviate from linearity with solute mole fraction.[32] Discontinuities in the concentration dependence of chemical shifts can reflect a change in the solvation number,[33] likely applicable to the inner coordination shell of Sn^{2+}.

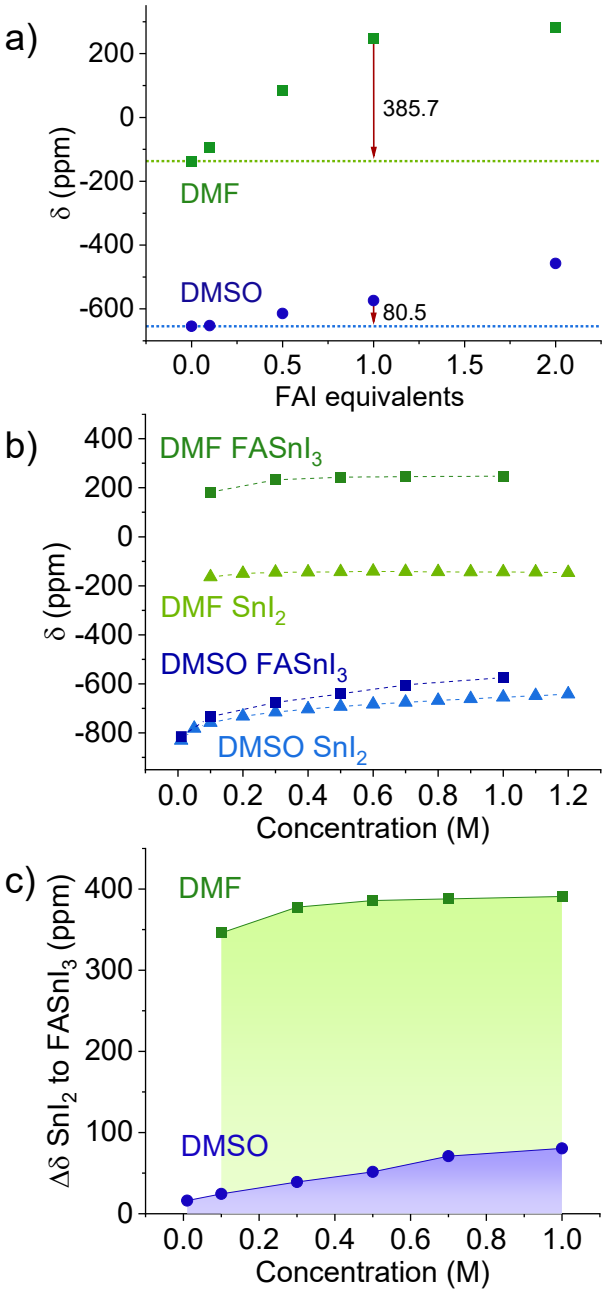

Figure 2. a) Chemical shift of ^{119}Sn NMR from SnI_2 in the presence of different stoichiometric values of FAI, and b) at different concentrations of SnI_2 and $FASnI_3$. SnI_2 data from our earlier work.[13] c) Change of chemical shift in ^{119}Sn NMR from SnI_2 to $FASnI_3$ at different concentrations.

In contrast, lead-based perovskites show different behavior with concentration in NMR (Figure S5).[34] In DMSO, the chemical shift of lead precursors increases with concentration, opposite to the decreasing trend observed in DMF. This effect has been reported by Maschwitz et al.,[35]

proposing that the iodidoplumbates increase their level of coordination when concentration increases, and thus the corresponding chemical shifts tend asymptotically from both sides to the solid-state $MAPbI_3$ value of 1423 ppm.[36] However, tin-based solutions (Figure 2b) fall far from the value of ~800 ppm found for $FASnI_3$ and $MASnI_3$ perovskites in solid-state NMR.[37] Furthermore, the values in both DMF and DMSO approach the solid-state chemical shift from more shielded positions, instead of converging from opposite directions, which suggests that overall, the same solvents have a stronger effect on their environment. In fact, the chemical shift greatly changes from PbI_2 to $MAPbI_3$ at any concentration and any solvent (Figure S6), unlike the case of SnI_2 to $FASnI_3$ in DMSO, which barely shows any change, illustrating the high affinity of this solvent to Sn^{2+}. Overall, NMR results point out the higher sensitivity of tin-based species to solution properties and processing conditions and enhanced solvation in the presence of strongly coordinating solvents or ligands.

The pronounced impact of solution composition on the metal species will inevitably affect their colloidal nature in the liquid state. To obtain a deeper sight on the structural organization and formation of PNCs in tin halide perovskites, we characterize these precursor solutions by SAXS using synchrotron radiation at BESSY II in Berlin, Germany, following our previous studies.[30, 34, 38] Further details and discussion in Supporting Information.

Data from Radicchi et al.[39] show that $FAPbI_3$ solutions exhibit a well-defined structure factor maximum at high q values in both DMF and DMSO, corresponding to a specific interparticle distance d depending on concentration. This effect manifests more strongly in DMF, where it appears at low concentrations (0.4 M), whereas in DMSO it emerges above 1.0 M. In $FASnI_3$ solutions, the structure factor becomes more diffuse in DMF and is even absent in DMSO (Figure 3a). Notably, SnI_2 solutions do not exhibit any structure factor maximum at any concentration (Figure S8). In DMF, the structure factor maximum shifts to higher q values with increasing concentration. Applying Bragg's law through the Laue condition in reciprocal space, $2\pi/q=d$, the q values correspond to a recurring interparticle distance d between the centers of mass (Pb^{2+}/Sn^{2+}) of 2.4 nm (0.4 M) decreasing to 1.6 nm (2.0 M) for $FAPbI_3$, and 1.9 nm decreasing to 1.3 nm for $FASnI_3$ (Figure 3b, S9, Table S5). These results suggest intensified interparticle interactions and increased colloidal stability (in line with increased repulsion forces) in perovskite solutions at higher molarity, which can be rationalized through the electric double layer (EDL) model.[30] The lower scattering intensity and broader structure factor peak

maximum for tin-based formulations suggest lower repulsion forces between the pristine perovskite subunits in the liquid and thus reduced colloidal stability in comparison, more prone to ad hoc and uncontrolled crystallization without undergoing intermediate formation. The higher *q* values of the structure factor maxima in $FASnI_3$ solutions relative to $FAPbI_3$ align with the expected larger size of lead-based PNCs and their longer interparticle distance. Meanwhile, DMSO completely suppresses the formation of a structure factor maximum, demonstrating its strong solvating role, but also its inability to stabilize a colloidal framework.

Unlike lead-based systems,[30, 34, 39] $FASnI_3$ solutions show increased intensity at low *q* values with a negative slope across all concentrations in both DMF and DMSO. This result suggests the coexistence of small particles and agglomerates, thus indicating a stronger tendency to evolve in an unordered manner. Dynamic light scattering measurements of $FAMI_3$ solutions agree with these observations and confirm the presence of PNCs (Figure S10). SnI_2 solutions exhibit similar behavior (Figure S8), indicating that the broad particle size distribution does not originate from the high chemical affinity of tin precursors with the A-site cation, but instead comes from the SnI_2 material itself, reinforcing the intrinsic predisposition of tin-based precursors toward inhomogeneous nucleation. Thus, while DMSO largely impedes perovskite precursor pre-arrangement in solution through strong solvation and effectively influences the crystallization process, as observed by NMR, it is ineffective in preventing the formation of agglomerates. Consequently, commonly employed Lewis base additives in tin-based solutions likely homogenize the nucleation process,[38] and do not necessarily, or mainly, induce grain coarsening as observed in lead perovskites.[35] In this regard, tuning the halide content in the tin-based perovskite composition could offer a simple and effective solution to manipulate the interparticle interactions as well as their tendency to agglomerate, as we previously proved for fluoride anions in the prevalent SnF_2 additive.[38]

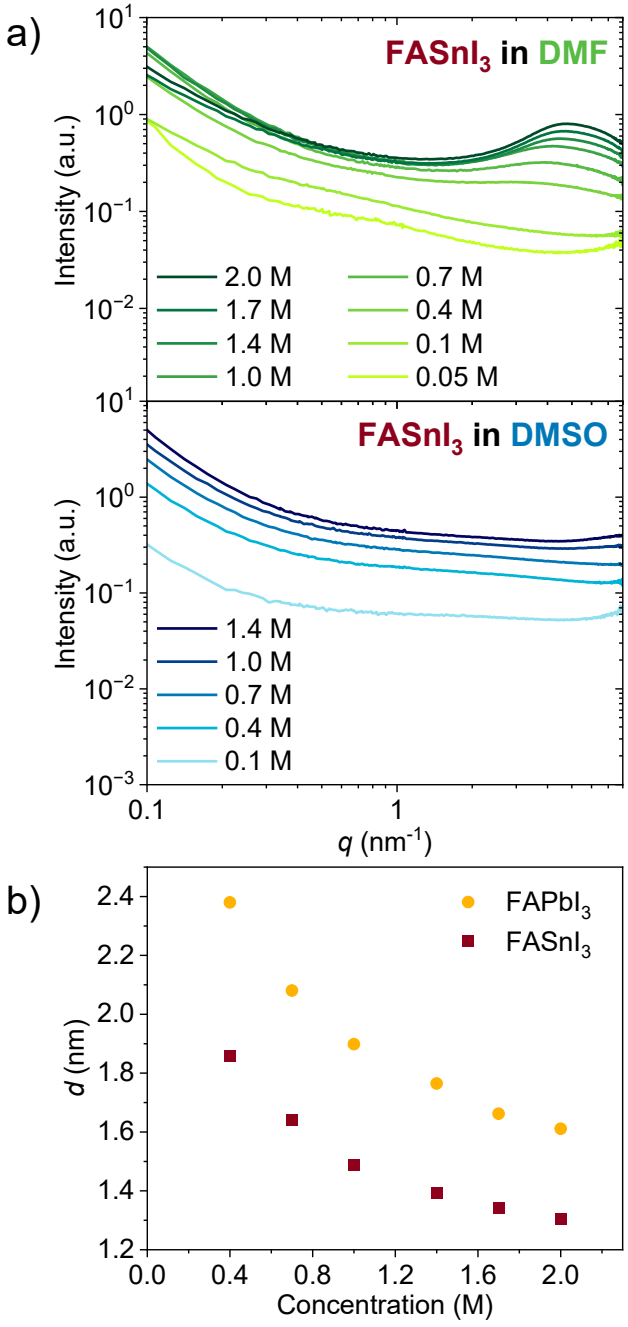

Figure 3. SAXS measurements. a) Patterns of $FASnI_3$ solutions in DMF and DMSO at different concentrations; b) mean interparticle distance *d* as a function of concentration in $FASnI_3$ solutions and $FAPbI_3$ data from Radicchi et al.[39]

In this work, we present a comparative analysis of the solution chemistry and colloidal behavior of lead- and tin-based perovskite precursor solutions, establishing the chemical

factors influencing distinct crystallization pathways. NMR and SAXS measurements allow us to identify the key differences that define the solution properties:

(i) Reactivity. Tin halides exhibit a higher affinity toward A-site salts than lead species, accelerating crystallization and narrowing the processing window for controlled nucleation and growth.

(ii) Sensitivity to conditions. The chemical environment of tin species shows pronounced susceptibility to changes in solution composition, in contrast to the more robust lead systems.

(iii) Colloidal properties. Tin precursor solutions display intrinsically lower colloidal stability than lead ones due to weaker interparticle repulsion, promoting agglomeration even in SnI_2 solutions and leading to inhomogeneous nucleation. These results, together with the direct conversion of Sn perovskites without intermediate stabilization, could infer that Sn perovskites would follow classical nucleation theory. However, the presence of PNCs and polydispersity in Sn-based solutions necessarily reveals a non-classical character, which, according to our observations, is strongly solvent-dependent. Figure 4 illustrates this through EDL and diffuse layer formation, highlighting solvent-dependent effects.

(iv) DMSO limitations. Although DMSO can partially moderate the reactivity of tin species with A-site salts, it fails to establish a stable colloidal environment and does not suppress aggregation despite its higher Sn^{2+} solvation (Figure 4). These unfavorable interactions with tin precursors help explain the limitations of DMSO-based protocols and highlight the potential of DMSO-free approaches[9, 26, 40-45] and alternative precursor preparation methods for more homogeneous solvation.[46-47]

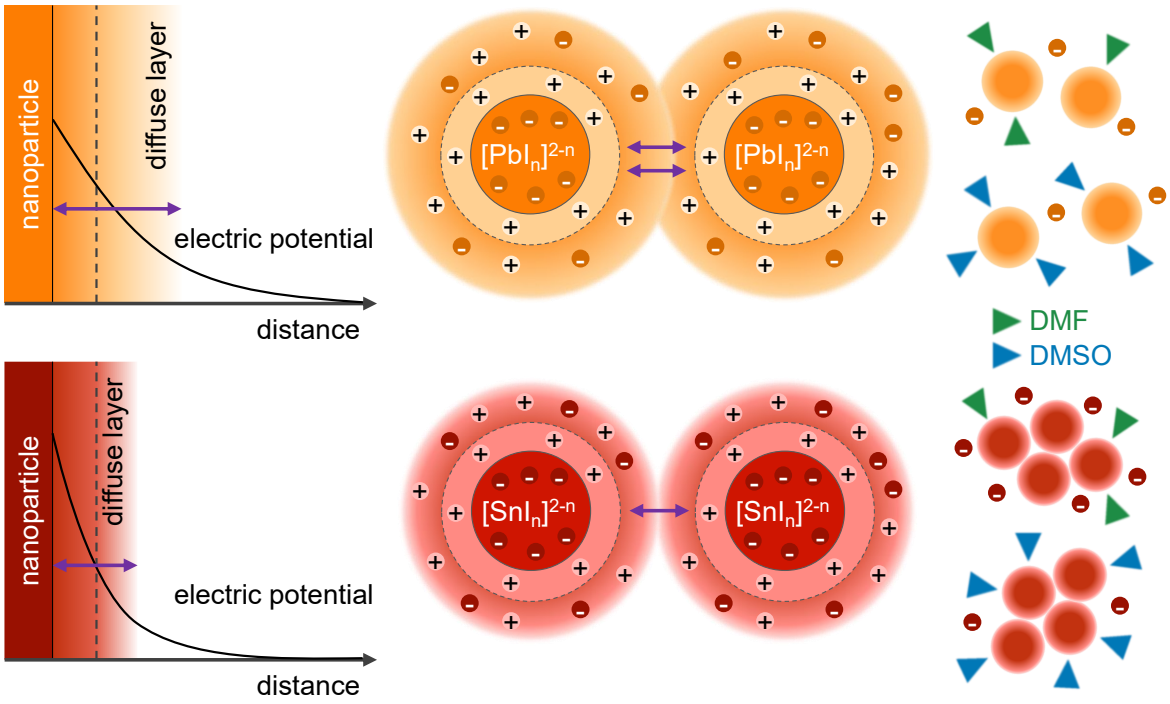

Figure 4. Less pronounced repulsion forces between Sn-based particles, reducing the stability of their colloidal system compared to Pb species and promoting their agglomeration.

The combined evidence reveals a unifying picture: tin perovskite precursor solutions are intrinsically more reactive and less colloidally stabilized than their lead counterparts. This fundamental difference results in a narrower processing window, where small variations in solvent coordination, precursor composition, or additives strongly influence nucleation and crystallization dynamics, explaining the difficulty of developing new protocols, device architectures and perovskite compositions.

From a practical perspective, these insights underscore the necessity of designing novel solvent systems that simultaneously moderate the high reactivity of Sn species while promoting a stable colloidal network. Recent DMSO-free strategies prove that this balance can be achieved through solvent combinations where a small fraction of strongly coordinating molecules solvates Sn^{2+} effectively, while a larger fraction of weakly coordinating solvents preserves colloidal organization.[9, 26, 40-45] Effective approaches must also suppress the intrinsic tendency of Sn precursors to agglomerate, where DMSO often fails. Additive engineering probably contributed to this direction, as we proved in the case of SnF_2[30, 34, 38] and the amino acid salts in the mixed tin-lead perovskite family.[11, 48]

Overall, this work provides a comprehensive description of the colloidal nature of tin halide perovskite precursors in comparison with conventional lead systems, offering fundamental guidance for rational precursor and solvent design to overcome current processing limitations and further advance tin-based perovskite solar cells and their related thin-film (opto)electronic devices.

SUPPORTING INFORMATION

Experimental details, NMR interpretation discussion, details on SAXS characterization, and a complete detailed list of NMR and SAXS data are available in the Supporting Information

ACKNOWLEDGMENTS

J.P. acknowledges support from Energy for the Future – E4F Postdoctoral Fellowship Program MSCA-COFUND (101034297). G.L. acknowledges the funding support from the National Natural Science Foundation of China (52503336) and Basic Research Program of Jiangsu (BK20251292).

REFERENCES

[1] M. Saliba, J.-P. Correa-Baena, M. Grätzel, A. Hagfeldt, A. Abate, *Angewandte Chemie International Edition* **2018**, *57*, 2554-2569.

[2] J.-P. Correa-Baena, M. Saliba, T. Buonassisi, M. Grätzel, A. Abate, W. Tress, A. Hagfeldt, *Science* **2017**, *358*, 739-744.

[3] X. Jiang, Z. Zang, Y. Zhou, H. Li, Q. Wei, Z. Ning, *Accounts of Materials Research* **2021**, *2*, 210-219.

[4] F. Hao, C. C. Stoumpos, R. P. H. Chang, M. G. Kanatzidis, *Journal of the American Chemical Society* **2014**, *136*, 8094-8099.

[5] M. T. Klug, R. L. Milot, J. B. Patel, T. Green, H. C. Sansom, M. D. Farrar, A. J. Ramadan, S. Martani, Z. Wang, B. Wenger, J. M. Ball, L. Langshaw, A. Petrozza, M. B. Johnston, L. M. Herz, H. J. Snaith, *Energy & Environmental Science* **2020**, *13*, 1776-1787.

[6] K. O. Ighodalo, W. Chen, Z. Liang, Y. Shi, S. Chu, Y. Zhang, R. Khan, H. Zhou, X. Pan, J. Ye, Z. Xiao, *Angewandte Chemie International Edition* **2023**, *62*, e202213932.

[7] A. Abate, *ACS Energy Letters* **2023**, *8*, 1896-1899.

[8] Z. Le, A. Liu, Y. Reo, S. Bai, Y.-Y. Noh, H. Zhu, *ACS Energy Letters* **2024**, *9*, 1639-1644.

[9] P. F. Sowmeeh, S. Zuo, C. Frasca, B. A. Seid, S. Ozen, W. Liu, M. H. Aldamasy, Y. Zhang, F. Zu, N. Koch, M. Stolterfoht, A. Abate, A. Musiienko, F. Lang, *ACS Energy Letters* **2025**, 6215-6222.

[10] S. Hu, J. Thiesbrummel, J. Pascual, M. Stolterfoht, A. Wakamiya, H. J. Snaith, *Chemical Reviews* **2024**, *124*, 4079-4123.

[11] S. Hu, J. Wang, P. Zhao, J. Pascual, J. Wang, F. Rombach, A. Dasgupta, W. Liu, M. A. Truong, H. Zhu, M. Kober-Czerny, J. N. Drysdale, J. A. Smith, Z. Yuan, G. J. W. Aalbers, N. R. M. Schipper, J. Yao, K. Nakano, S. H. Turren-Cruz, A. Dallmann, M. G. Christoforo, J. M. Ball, D. P. McMeekin, K. A. Zaininger, Z. Liu, N. K. Noel, K. Tajima, W. Chen, M. Ehara, R. A. J. Janssen, A. Wakamiya, H. J. Snaith, *Nature* **2025**, *639*, 93-101.

[12] L. Lanzetta, T. Webb, N. Zibouche, X. Liang, D. Ding, G. Min, R. J. E. Westbrook, B. Gaggio, T. J. Macdonald, M. S. Islam, S. A. Haque, *Nature Communications* **2021**, *12*, 2853.

[13] J. Pascual, G. Nasti, M. H. Aldamasy, J. A. Smith, M. Flatken, N. Phung, D. Di Girolamo, S.-H. Turren-Cruz, M. Li, A. Dallmann, R. Avolio, A. Abate, *Materials Advances* **2020**, *1*, 1066-1070.

[14] N. K. Noel, S. D. Stranks, A. Abate, C. Wehrenfennig, S. Guarnera, A.-A. Haghighirad, A. Sadhanala, G. E. Eperon, S. K. Pathak, M. B. Johnston, A. Petrozza, L. M. Herz, H. J. Snaith, *Energy & Environmental Science* **2014**, *7*, 3061-3068.

[15] F. Hao, C. C. Stoumpos, D. H. Cao, R. P. H. Chang, M. G. Kanatzidis, *Nature Photonics* **2014**, *8*, 489-494.

[16] F. Hao, C. C. Stoumpos, P. Guo, N. Zhou, T. J. Marks, R. P. H. Chang, M. G. Kanatzidis, *Journal of the American Chemical Society* **2015**, *137*, 11445-11452.

[17] J. Wang, Z. Gao, J. Yang, M. Lv, H. Chen, D.-J. Xue, X. Meng, S. Yang, *Advanced Energy Materials* **2021**, *11*, 2102131.

[18] J.-J. Cao, Y.-H. Lou, K.-L. Wang, Z.-K. Wang, *Journal of Materials Chemistry C* **2022**, *10*, 7423-7436.

[19] M. Yin, H. Yao, H. Qiu, C. Wu, M. Zhang, F. Hao, *Advanced Functional Materials* **2024**, *34*, 2404792.

[20] M. Qin, P. F. Chan, X. Lu, *Advanced Materials* **2021**, *33*, 2105290.

[21] G. Li, Z. Su, M. Li, F. Yang, M. H. Aldamasy, J. Pascual, F. Yang, H. Liu, W. Zuo, D. Di Girolamo, Z. Iqbal, G. Nasti, A. Dallmann, X. Gao, Z. Wang, M. Saliba, A. Abate, *Advanced Energy Materials* **2021**, *11*, 2101539.

[22] O. E. Solis, M. Mínguez-Avellán, P. F. Betancur, R. I. Sánchez- Alarcón, I. Rodriguez, J. P. Martínez-Pastor, T. S. Ripolles, R. Abargues, P. P. Boix, *ACS Energy Letters* **2024**, *9*, 5288-5295.

[23] D. He, P. Chen, J. A. Steele, Z. Wang, H. Xu, M. Zhang, S. Ding, C. Zhang, T. Lin, F. Kremer, H. Xu, M. Hao, L. Wang, *Nature Nanotechnology* **2025**, *20*, 779-786.

[24] D. Amoroso, G. Nasti, M. M. Villone, T. Kodalle, C. M. Sutter-Fella, P. L. Maffettone, A. Abate, *ACS Energy Letters* **2025**, *10*, 5781-5787.

[25] A. Abate, *Nature Nanotechnology* **2025**, *20*, 719-720.

[26] J. Pascual, D. Di Girolamo, M. A. Flatken, M. H. Aldamasy, G. Li, M. Li, A. Abate, *Chemistry – A European Journal* **2022**, *28*, e202103919.

[27] X. Yang, T. Ma, H. Hu, W. Ye, X. Li, M. Li, A. Zhang, C. Ge, X. Sun, Y. Zhu, S. Yan, J. Yan, Y. Zhou, Z. a. Li, C. Chen, H. Song, J. Tang, *Nature Photonics* **2025**, *19*, 426-433.

[28] E. Radicchi, E. Mosconi, F. Elisei, F. Nunzi, F. De Angelis, *ACS Applied Energy Materials* **2019**, *2*, 3400-3409.

[29] J. Kim, B.-w. Park, J. Baek, J. S. Yun, H.-W. Kwon, J. Seidel, H. Min, S. Coelho, S. Lim, S. Huang, K. Gaus, M. A. Green, T. J. Shin, A. W. Y. Ho-baillie, M. G. Kim, S. I. Seok, *Journal of the American Chemical Society* **2020**, *142*, 6251-6260.

[30] M. A. Flatken, E. Radicchi, R. Wendt, A. G. Buzanich, E. Härk, J. Pascual, F. Mathies, O. Shargaieva, A. Prause, A. Dallmann, F. De Angelis, A. Hoell, A. Abate, *Chemistry of Materials* **2022**, *34*, 1121-1131.

[31] S. Hu, J. Wang, P. Zhao, J. Pascual, J. Wang, F. Rombach, A. Dasgupta, W. Liu, M. A. Truong, H. Zhu, M. Kober-Czerny, J. N. Drysdale, J. A. Smith, Z. Yuan, G. J. W. Aalbers, N. R. M. Schipper, J. Yao, K. Nakano, S.-H. Turren-Cruz, A. Dallmann, M. G. Christoforo, J. M. Ball, D. P. McMeekin, K.-A. Zaininger, Z. Liu, N. K. Noel, K. Tajima, W. Chen, M. Ehara, R. A. J. Janssen, A. Wakamiya, H. J. Snaith, *Nature* **2025**, *639*, 93-101.

[32] J. F. Coetzee, C. D. Ritchie, *Solute-solvent interactions*, New York, M. Dekker, **1969**.

[33] J. Burguess, *Metal ions in solution*, Ellis Horwood Ltd. Chichester, **1978**.

[34] M. A. Flatken, A. Hoell, R. Wendt, E. Härk, A. Dallmann, A. Prause, J. Pascual, E. Unger, A. Abate, *Journal of Materials Chemistry A* **2021**, *9*, 13477-13482.

[35] T. Maschwitz, L. Merten, F. Ünlü, M. Majewski, F. Haddadi Barzoki, Z. Wu, S. D. Öz, C. Kreusel, M. Theisen, P. Wang, M. Schiffer, G. Boccarella, G. Marioth, H. Weidner, S. Schultheis, T. Schieferstein, D. Gidaszewski, Z. Julliev, E. Kneschaurek, V. Munteanu, I. Zaluzhnyy, F. Bertram, A. Jaffrès, J. He, N. Ashurov, M. Stolterfoht, C. M. Wolff, E. Unger, S. Olthof, G. Brocks, S. Tao, H. Grüninger, O. J. J. Ronsin, J. Harting, A. F. Kotthaus, S. F. Kirsch, S. Mathur, A. Hinderhofer, F. Schreiber, T. Riedl, K. O. Brinkmann, *Nature Communications* **2025**, *16*, 9894.

[36] C. Roiland, G. Trippé-Allard, K. Jemli, B. Alonso, J.-C. Ameline, R. Gautier, T. Bataille, L. Le Pollès, E. Deleporte, J. Even, C. Katan, *Physical Chemistry Chemical Physics* **2016**, *18*, 27133-27142.

[37] D. J. Kubicki, D. Prochowicz, E. Salager, A. Rakhmatullin, C. P. Grey, L. Emsley, S. D. Stranks, *Journal of the American Chemical Society* **2020**, *142*, 7813-7826.

[38] J. Pascual, M. Flatken, R. Félix, G. Li, S.-H. Turren-Cruz, M. H. Aldamasy, C. Hartmann, M. Li, D. Di Girolamo, G. Nasti, E. Hüsam, R. G. Wilks, A. Dallmann, M. Bär, A. Hoell, A. Abate, *Angewandte Chemie International Edition* **2021**, *60*, 21583-21591.

[39] E. Radicchi, M. A. Flatken, A. Hoell, E. Mosconi, W. Kaiser, J. Pascual, W. Liu, A. Dallmann, A. Abate, F. De Angelis, *Submitted* **2025**.

[40] D. Di Girolamo, J. Pascual, M. H. Aldamasy, Z. Iqbal, G. Li, E. Radicchi, M. Li, S.-H. Turren-Cruz, G. Nasti, A. Dallmann, F. De Angelis, A. Abate, *ACS Energy Letters* **2021**, *6*, 959-968.

[41] G. Nasti, M. H. Aldamasy, M. A. Flatken, P. Musto, P. Matczak, A. Dallmann, A. Hoell, A. Musiienko, H. Hempel, E. Aktas, D. Di Girolamo, J. Pascual, G. Li, M. Li, L. V. Mercaldo, P. D. Veneri, A. Abate, *ACS Energy Letters* **2022**, *7*, 3197-3203.

[42] H. Rao, Y. Su, G. Liu, H. Zhou, J. Yang, W. Sheng, Y. Zhong, L. Tan, Y. Chen, *Angewandte Chemie International Edition* **2023**, *62*, e202306712.

[43] S. Zuo, A. Tarasov, L. Frohloff, K. Prashanthan, F. Ruske, M. Lounasvuori, C. Frasca, A. Dallmann, F. Zu, F. Mathies, F. Scheler, N. T. P. Hartono, G. Li, J. Li, M. Simmonds, W. Li, N. Koch, S. Albrecht, M. Li, E. Unger, M. H. Aldanmasy, A. Musiienko, A. Abate, *Advanced Science* **2025**, *12*, e01311.

[44] D. P. Panda, R. Issaoui, Z. Iqbal, G. K. Grandhi, M. O. Ur Rehman, F. Zu, P. Alippi, M. Rastgoo, S. Zuo, E. Luzzi, M. Simmonds, L. Miele, L. Sanguigno, M. Li, P. Aprea, E. Di Maio, N. Koch, P. Vivo, A. Abate, *ACS Energy Letters* **2025**, *10*, 3789-3798.

[45] F. Harata, R. Kaneko, S. Hu, N. Ohashi, T. Nakamura, M. A. Truong, R. Murdey, A. Wakamiya, *ACS Energy Letters* **2025**, *10*, 5047-5056.

[46] X. Jiang, H. Li, Q. Zhou, Q. Wei, M. Wei, L. Jiang, Z. Wang, Z. Peng, F. Wang, Z. Zang, K. Xu, Y. Hou, S. Teale, W. Zhou, R. Si, X. Gao, E. H. Sargent, Z. Ning, *Journal of the American Chemical Society* **2021**, *143*, 10970-10976.

[47] M. Ozaki, Y. Katsuki, J. Liu, T. Handa, R. Nishikubo, S. Yakumaru, Y. Hashikawa, Y. Murata, T. Saito, Y. Shimakawa, Y. Kanemitsu, A. Saeki, A. Wakamiya, *ACS Omega* **2017**, *2*, 7016-7021.

[48] S. Hu, X. Sun, W. Liu, L. Gregori, P. Zhao, J. Pascual, A. Dallmann, A. Dasgupta, F. Yang, G. Li, M. Aldamasy, S.-H. Turren-Cruz, M. A. Flatken, S. Fu, Y. Iwasaki, R. Murdey, A. Hoell, S. Schorr, S. Albrecht, S. Yang, A. Abate, A. Wakamiya, F. De Angelis, M. Li, H. J. Snaith, *Angewandte Chemie International Edition* **2025**, *64*, e202514010.